TR-0311

AD

Reports Control Symbol
OSD - 1366

ENERGY BALANCE MODEL FOR IMAGERY AND ELECTROMAGNETIC PROPAGATION

May 1992

Henry Rachele
Arnold Tunick

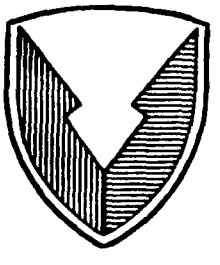

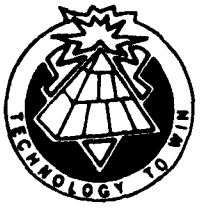

Approved for public release; distribution is unlimited.

US ARMY
LABORATORY COMMAND
ATMOSPHERIC SCIENCES LABORATORY
White Sands Missile Range, NM 88002-5501

NOTICES

Disclaimers

The findings in this report are not to be construed as an official Department of the Army position, unless so designated by other authorized documents.

The citation of trade names and names of manufacturers in this report is not to be construed as official Government indorsement or approval of commercial products or services referenced herein.

Destruction Notice

When this document is no longer needed, destroy it by any method that will prevent disclosure of its contents or reconstruction of the document.

REPORT DOCUMENTATION PAGE

Form Approved
OMB No. 0704-0188

1. AGENCY USE ONLY (Leave blank)	2. REPORT DATE	3. REPORT TYPE AND DATES COVERED
	May 1992	Final

4. TITLE AND SUBTITLE
Energy Balance Model for Imagery and Electromagnetic Propagation

5. FUNDING NUMBERS
DA Task
B-53A-B 611102.53A 40.11

6. AUTHOR(S)
Henry Rachele and Arnold Tunick

7. PERFORMING ORGANIZATION NAME(S) AND ADDRESS(ES)
U.S. Army Atmospheric Sciences Laboratory
White Sands Missile Range, NM 88002-5501

8. PERFORMING ORGANIZATION REPORT NUMBER
ASL-TR-0311

9. SPONSORING/MONITORING AGENCY NAME(S) AND ADDRESS(ES)
U.S. Army Laboratory Command
Adelphi, MD 20783-1145

10. SPONSORING/MONITORING AGENCY REPORT NUMBER

11. SUPPLEMENTARY NOTES

12a. DISTRIBUTION/AVAILABILITY STATEMENT
Approved for public release; distribution is unlimited.

12b. DISTRIBUTION CODE

13. ABSTRACT (Maximum 200 words)

The optical turbulence structure parameter C_n^2 typically appears in formulations used to estimate the effects of temperature and moisture (gradients) on imagery and electromagnetic propagation. Temperature and moisture gradients can be approximated from sensible and latent heat flux estimates, and these fluxes can be obtained from radiation/energy balance equations. Numerous energy balance models exist requiring different kinds and numbers of inputs. The semiempirical model developed and presented in this report was constrained to require a minimum number of conventional measurements at a reference level (2 m). These measurements include temperature, pressure, relative humidity, and windspeed. The model also requires a judgment of soil type and moisture (dry, moist, or saturated), cloud characteristics (tenths of cloud cover and density and an estimate of cloud height), day of the year, time of day, and longitude and latitude of the site of interest. Model estimates of net radiation, sensible and latent heat fluxes and C_n^2 are compared with measured values.

14. SUBJECT TERMS	15. NUMBER OF PAGES
Radiation/energy balance, net radiation, sensible heat flux, latent heat flux, ground heat flux, Similarity Theory, optical structure parameter C_n^2	39
	16. PRICE CODE

17. SECURITY CLASSIFICATION OF REPORT	18. SECURITY CLASSIFICATION OF THIS PAGE	19. SECURITY CLASSIFICATION OF ABSTRACT	20. LIMITATION OF ABSTRACT
Unclassified	Unclassified	Unclassified	SAR

ACKNOWLEDGMENT

We thank Frank V. Hansen of ASL for his willing and enthusiastic support and encouragement during the development of the model. He not only searched out many pertinent documents but also gave his time for discussion.

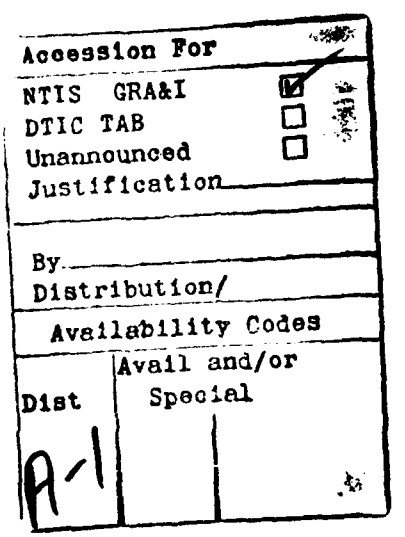

CONTENTS

LIST OF ILLUSTRATIONS

Figures

TABLES

1. INTRODUCTION

The optical turbulence structure parameter C_n^2 appears in formulations used to estimate the effects of atmospheric turbulence on imagery and electromagnetic (EM) propagation. For many optical systems C_n^2 corresponds with degradation of performance (Miller and Ricklin 1990; Tatarski 1961; Fried 1967). Basic formulations of C_n^2 (Panofsky 1968; Tatarski 1961; Hill 1989; Andreas 1988; Wyngaard 1973; Wesley 1976; Tunick and Rachele 1992) include the gradient of the real index of refraction as a coefficient, which in turn, is a function of the gradients of temperature and moisture (preferably potential temperature and specific humidity according to Tatarski (1961)). Temperature and moisture gradients can be approximated from sensible and latent heat flux estimates, and these fluxes can be obtained from radiation/energy balance formations.

Numerous radiation/energy balance models appear in the literature (Angus-Leppan and Brunner 1980; Webb 1984; Campbell 1985; Pielke 1984; Danard et al. 1984; Yamada 1981; Carson 1987, to name a few) varying from comparatively simple to academically complex and requiring different amounts and numbers of inputs and computer capabilities. In this report we present a model (hereafter known as the RT model) that was developed for imaging and EM propagation applications when a minimum of atmospheric information is available. This report provides the concept and formulations that make up the first formalized version of the model. Other reports will follow as the model evolves.

The primary outputs of the RT model are estimates of sensible and latent heat fluxes, which in turn, are used for estimating gradients of potential temperature and specific humidity, making use of similarity relations. These gradients are then used to estimate the optical turbulence parameter C_n^2 needed in the imaging and propagation equations.

The remainder of this report is structured into the following sections: Model Concept, Model Equations, Computation Procedure, Sample Results, Summary and Conclusions, and Literature Cited.

2. MODEL CONCEPT

The model concept is a fallout from the operational scenario as follows. One is interested in estimating the optical turbulence C_n^2 at a temporary site for different times of one day. The day of interest is known, and the longitude and latitude of the site are known. From geological maps one knows the soil composition; and from the meteorological reports one has an estimate of soil wetness; that is, dry, moist, or wet. However, if the geological and meteorological reports are not available, one makes on-the-spot judgments by examining samples of soil from the surface to 10 cm below the surface. In addition to the soil judgment, one also makes a judgment of sky conditions; in particular, the amount of cloud cover (in tenths from 0 to 1), an estimation of cloud height, and the density of the clouds (0 to 3). From the above information one proceeds to estimate the sensible and latent heat fluxes by using the convention and formulations of radiation and energy balance proposed by Carson (1987) as discussed below.

2.1 Radiation Balance Concepts

Carson (1987) states that the net radiation flux R_N at the soil surface is equal to the sum of the net short-wave radiative flux, R_{SN}, and the net long-wave radiative flux, R_{LN}; that is,

$$R_N = R_{SN} + R_{LN} . \tag{1}$$

The short- and long-wave fluxes are illustrated in figure 1.

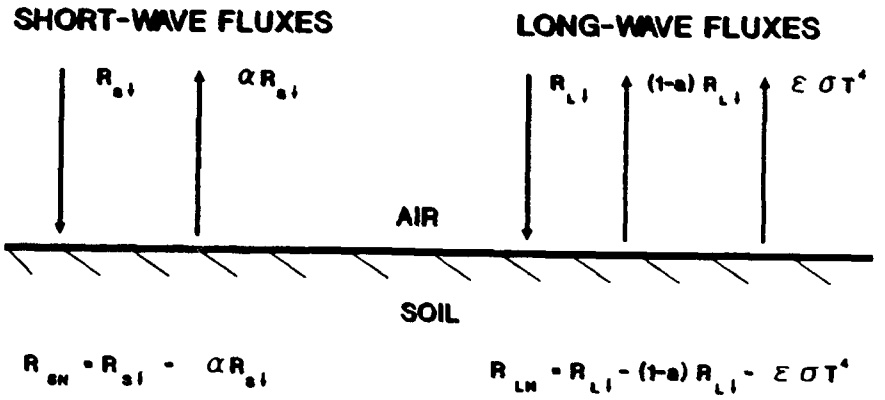

Figure 1. Schematic representation of short-wave and long-wave radiative fluxes at a bare-soil surface.

In figure 1 $R_{S\downarrow}$ is the downward short-wave radiative flux (including both the direct solar flux and diffuse radiation from the sky). However, some of the short-wave radiation is reflected at the earth's surface so that

$$R_{SN} = R_{S\downarrow} - \alpha R_{S\downarrow} , \tag{2}$$

where α is the surface short-wave reflectivity, commonly called albedo. However, albedo is not as simple as it appears in equation (2); it is a function of soil type, color, vegetative cover and the elevation angle of the sun. Values of α as a function of soil and vegetation are given in table 1, mainly from Danard et al. (1984) and Campbell (1977); the functional form of α relative to the sun's position is given in section 3 (equation (20)).

Carson (1987) also notes that if $R_{L\downarrow}$ is the downward long-wave radiation and a is the surface absorptivity to long-wave radiation, then the net incoming flux from the atmosphere is $(a\, R_{L\downarrow})$. Using Stefan's law, one can write that the upward flux due to thermal emission at the earth's surface is $\epsilon\, \sigma\, T_g^4$, where T_g is the effective surface temperature, ϵ is the long-wave emissivity at the surface, and σ is the Stefan-Boltzman constant. Hence, the net long-wave radiative flux, R_{LN}, is

$$R_{LN} = a\, R_{L\downarrow} - \epsilon\, \sigma\, T_g^4 . \tag{3}$$

TABLE 1. TYPICAL VALUES OF ALBEDO, α, AND EMISSIVITY, ϵ, FOR VARIOUS SURFACES*

Surface	α	ϵ
O'Neill average (D)	0.25	0.90
Clay pasture (D)	0.15	0.95
Dry Clay (G)		
Wet Clay (G)		
Sandy clay (15% moisture) (J)		
Dry quartz sand (D)	0.40	0.80
Dry sand (G)		
Wet sand (G)		
Dry moorland (G)		
Wet moorland (G)		
Rock (G)		
Ice (G,M)	0.65	0.97
Snow (D,M)	0.65	
New snow (G,DGL)	0.85	
Old snow (G,DGL)	0.30	

D: Deardorff (1978)**
DGL: Danard et al. (1984)**
G: Geiger (1961, p. 29)**
J: Johnson (1954, p. 156)**
M: Mellor (1977)**

From Campbell (1977)***

Surface	α	Surface	α
Grass	0.24	Deciduous woodland	0.18
Wheat	0.26	Coniferous woodland	0.16
Maize	0.22	Swamp forest	0.12
Pineapple	0.15	Open water	0.05
Sugar Cane	0.15	Dry soil (light color)	0.32

*M. Danard, G. Lyv, and G. MacGillivray, A Mesoscale Bulk Model of the Atmospheric Boundary Layer, Atmospheric Dynamics Corporation report, Victoria, British Columbia, Canada, 1984.

**Complete reference information is contained in Danard, Lyv, and MacGillivray.

***G. S. Campbell, An Introduction to Environmental Biophysics, Springer Verlag, New York, 1977.

It is common practice to combine the definition of ϵ with Kirchhoff's law so that $a = \epsilon$. However, ϵ varies with soil type, vegetation, and snow or water cover as given in table 1.

2.2 Surface Energy Flux Balance Concepts

Carson (1987) writes the energy flux balance at the soil surface as

$$R_N = H + L'E + G_g \ , \tag{4}$$

where R_N is the net radiative flux, H is the turbulent sensible-heat flux, $L'E$ is the latent-heat flux due to surface evaporation, and G_g is the flux of heat into the soil. The convention of equation (4) is shown in figure 2.

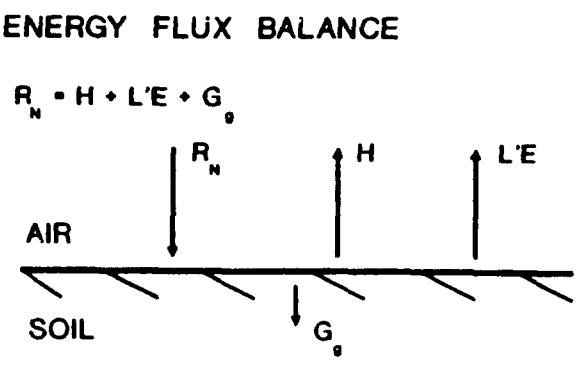

Figure 2. Schematic representation of the energy flux balance at a bare-soil surface.

Equations for H, $L'E$, *and* G_g are given in section 3. Having established the basic radiation/energy balance formulations and their directional conventions, we now discuss the equations chosen to evaluate them. There are a multitude of relations to choose from.

3. EQUATIONS

3.1 Short-Wave Solar Radiation

The formulations we use to compute the incoming short-wave solar radiation for cloudless skies are patterned after Meyers and Dale (1983) and Miller and Ricklin (1990). These are then augmented with empirical results by Haurwitz (1945) to account for cloudy skies.

For clear skies Meyers and Dale (1983) write

$$R_{S\downarrow} = I = I_o \, T_R \, T_g \, T_w \, T_a \cos Z \ , \tag{5}$$

where I_o is the extraterrestrial flux density at the top of the atmosphere on a surface normal to the incident radiation, Z the solar zenith angle, and T_i are the transmission coefficients for Rayleigh scattering (R), absorption by permanent gases (g), water vapor (w), and absorption and scattering of aerosols (a).

I_o changes throughout the year because of changes in the earth-sun distance and is adjusted by using the equation

$$I_o = 1353\ (W\ m^{-2}) \left\{ 1 + 0.034 \cos \left[2\pi\ (n' - 1)\ /\ 365 \right] \right\}, \tag{6}$$

where n′ is the Julian day. The solar zenith angle is computed by using

$$Z = \cos^{-1} \left\{ \sin(\delta) \sin(D) + \cos(\delta) \cos(D) \cos(H') \right\}, \tag{7}$$

where δ is the latitude, D the declination angle, and H' is the solar hour angle. Miller and Ricklin (1990) compute the solar declination angle using formulations by Woolf (1968)

$$\sin D = \sin(23.4438) \sin \beta, \tag{8}$$

where β, in degrees, is

$$\beta = \gamma + 0.4087 \sin(\gamma) + 1.8724 \cos(\gamma) - 0.0182 \sin(2\gamma) + 0.0083 \cos(2\gamma), \tag{9}$$

and γ, in degrees, is

$$\gamma = 279.9348 + d\ . \tag{10}$$

The angle d is the angular fraction of a year represented by a particular date. The angle d may be calculated by

$$d = (\textit{number of day of year} - 1)\ (360/365.242)\ . \tag{11}$$

The solar hour angle H', in degrees, is a measure of the longitudinal distance from the sun to the point of calculations given by

$$H' = 15\ (T - M) - \eta\ , \tag{12}$$

where T is the Greenwich mean time (GMT) of the calculations, M is the time in hours after midnight of the passage of the sun over the Greenwich meridian or true solar noon, and η is longitude, counted positive west of Greenwich. In terms of d defined in equation (11), M is

$$M = 12.0 + 0.12357 \sin(d) - 0.004289 \cos(d) + 0.153809 \sin(2d) + 0.060783 \cos(2d) \tag{13}$$

An empirical equation for $T_R\ T_g$ in equation (5) by Kondartyev (1969) and modified by Atwater and Brown (1974) to include forward scattering is

$$T_R\ T_g = 1.021 - 0.084 \left[m\ (949\ P \times 10^{-5} + 0.051) \right]^{1/2}, \tag{14}$$

where P is the surface pressure (kPa), and m is the optical air mass at a pressure of 101.3 kPa given by

$$m = 35\ (1224\ \cos^2\ (Z) + 1)^{-1/2},\ \textit{where Z is the zenith angle.} \qquad (15)$$

An expression for computing the broad-band transmission of water vapor absorption by McDonald (1960) is

$$T_w = 1 - 0.077\ (um)^{0.3}\ , \qquad (16)$$

where m is the optical air mass (defined above) and u, the precipitable water vapor, is determined by using an expression by Smith (1966); that is,

$$u = \frac{P_r\ W_r}{g\ (\lambda + 1)}\ , \qquad (17)$$

where P_r is the pressure at the earth's surface, W_r is the mixing ratio, g is the acceleration due to gravity, and λ is given in table 2.

TABLE 2. SEASONAL AND LATITUDINAL MEAN VALUES OF λ

Season Latitudinal Zone (deg N)	Winter	Spring	Summer	Fall	Annual Average
0-10	3.37	2.85	2.80	2.64	2.91
10-20	2.99	3.02	2.70	2.93	2.91
20-30	3.60	3.00	2.98	2.93	3.12
30-40	3.04	3.11	2.92	2.94	3.00
40-50	2.70	2.95	2.77	2.71	2.78
50-60	2.52	3.07	2.67	2.93	2.79
60-70	1.76	2.69	2.61	2.61	2.41
70-80	1.60	1.67	2.24	2.63	2.03
80-90	1.11	1.44	1.94	2.02	1.62
Northern Hemisphere average	2.52	2.64	2.62	2.70	2.61

A simple treatment used by Meyers and Dale (1983) for estimating T_a was proposed by Houghton (1954)

$$T_a = X^m\ , \qquad (18)$$

where m is the optical mass, and X is an empirically derived constant (on the order of 0.935).

To account for the effect of clouds we introduce a transmission coefficient T_c derived empirically by Haurwitz (1945, 1946, 1948). Haurwitz (1945) chose to express T_c by

$$T_c = \frac{aa}{m}\ e^{-bm}\ . \qquad (19)$$

where aa and b are constants whose values were determined by using least square techniques applied to observed clouds of different percentage sky cover and of varying density. He also computed the ratio of insolation with partly or completely covered sky to insolation of cloudless skies as shown in table 3.

TABLE 3. RATIO OF INSOLATION WITH PARTLY OR COMPLETELY CLOUD-COVERED SKY TO THE INSOLATION WITH CLOUDLESS SKY IN PERCENT

Cloud Amount Tenths	1-3				4-7			8-9			10				
Air Mass/ Density	0	1	2	3	1	2	3	1	2	3	0	1	2	3	4
1.0	104	103	98	88	98	93	88	92	76	68	87	80	60	31	18
1.5	99	100	97	90	96	89	83	92	75	65	88	79	58	30	19
2.0	94	98	96	92	94	85	78	92	75	63	88	79	55	28	20
2.5	90	96	94	94	92	81	74	92	74	60	89	79	52	27	20
3.0	85	94	92	96	90	78	69	93	74	58	89	79	50	27	21
3.5	81	92	90	98	87	74	65	93	73	56	90	79	47	25	21
4.0	77	90	89	100	84	71	61	93	72	54	90	79	46	25	22
4.5	73	88	87	102	82	67	58	93	72	52	91	79	44	24	23
5.0	70	86	85	104	80	64	54	93	72	50	91	79	41	23	23

We use table 3 to correct our estimates of insolation for cloud cover.

At this point we have formulations for computing the incoming short-wave solar radiation $R_{S\downarrow}$, which is then adjusted for albedo. As indicated in table 1, albedo is a function of soil type, color, moisture, vegetation, and solar elevation angle. Although the first four effects are reflected in table 1, the last is computed by using an approximation by Paltridge and Platt (1976); that is,

$$\alpha(Z) = \alpha_1 + (1 - \alpha_1) \exp\left[-k\ (90^\circ - Z)\right], \tag{20}$$

where k is of order 0.1, Z is the solar zenith angle, and α_1 is the small zenith angle value of albedo.

3.2 Upward Long-Wave Radiation

The upward long-wave radiative flux $R_{L\uparrow}$ is computed by using a formulation from Yamada (1981).

$$R_{L\uparrow} = \epsilon_g\ \sigma\ T_g^4 + (1 - \epsilon_g)\ R_{L\downarrow}\ , \tag{21}$$

where ϵ_g is the surface emissivity (see table 1), and σ is the Stefan-Boltzman constant. To evaluate equation (21) one requires an estimate of the effective ground temperature T_g.

This is done as follows: We assume that a semiempirical expression of the sensible heat flux, H, given by Angus-Leppan (1971) (based on the Penman (1948) combination form) is adequate as a first approximation for clear sky dry ground conditions. Angus-Leppan's expression is

$$H = 450\ C\ W \sin \phi_e\ , \tag{22}$$

where C and W are correction factors (see figure 3 for the amount of cloud cover and ground wetness, respectively), and ϕ_e is the solar elevation angle ($\phi_e = 90 - Z$). For clear skies and dry ground C = W = 1 in equation (22).

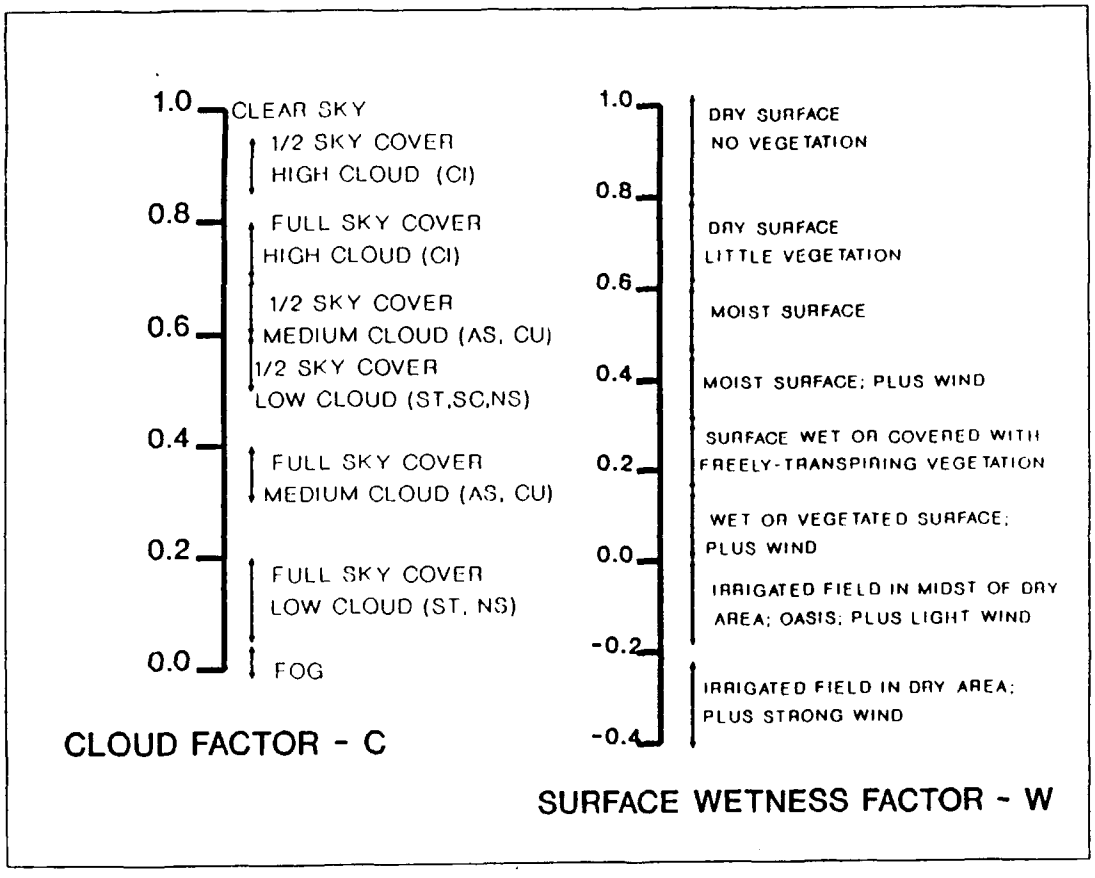

Figure 3. Estimation of parameters C and W.

Having an estimate for H, equation (22), we compute the similarity forms for the Monin-Obukhov length L and friction velocity u* using

$$L = \frac{-u^{*3} C_p \rho \theta_{vr}}{kgH} \tag{23}$$

where C_p is the specific heat of air, ρ is the density of air, θ_{vr} is the reference level potential temperature, k is Karman's constant (0.4), and g is acceleration due to gravity.

$$u^* = V_r k \left[\left\{ \ln \left(\frac{x - 1}{x + 1} \right) + 2 \tan^{-1} x \right\} \Big|_{zo}^{z-d} \right]^{-1}, \tag{24}$$

where $x = (1 - 15 \frac{z}{L})^{1/4}$ for neutral and unstable conditions, and $x = 1 + 5 \frac{z}{L}$ for stable conditions.

Solving equations (23) and (24) iteratively we obtain values for L and u* for the approximated value of H. Also, from similarity forms we can write

$$\theta^* = \frac{u^{*2}\,\theta_{vr}}{kgL} \quad . \tag{25}$$

Hence, we can compute a first estimate for θ^*, which can be used to approximate T_g since

$$T_g = T(z) - \frac{\theta^*}{k}\left\{\ln\left(\frac{y-1}{y+1}\right)\right\}\Big|_{z_h}^{z-d} \tag{26}$$

where $y = (1 - 15\,\frac{z}{L})^{1/2}$ for neutral and unstable conditions, and $y = 1 + 5\,\frac{z}{L}$ for stable conditions.

However, to evaluate equation (26) we require an estimate of Z_h (the roughness length for temperature), which is determined from our modification of Verma (1989); that is,

$$Z_h = \frac{L}{15}\left\{1 - \left(\frac{1+B^*}{1-B^*}\right)^2\right\}, \tag{27}$$

where

$$B^* = \left(\frac{y(z-d)+1}{y(z-d)-1}\right) e^{(kB^{-1}+A)}, \tag{28}$$

$$A = \left\{\ln\left(\frac{x-1}{x+1}\right) + 2\tan^{-1}.x\right\}\Big|_{z_o}^{z-d}; \tag{29}$$

$$Y = \left(1 - 15\,\frac{Z}{L}\right)^{1/2}; \tag{30a}$$

$$X = \left(1 - 15\,\frac{Z}{L}\right)^{1/4} . \tag{30b}$$

Z_o = roughness length for momentum.

B = Stanton number.

k = Karman's constant (0.4).

Values for kB^{-1} for different soil surfaces and vegetation are given in figure 4. Having an estimate of T_g for dry cloudless conditions we compute $R_{L\uparrow}$.

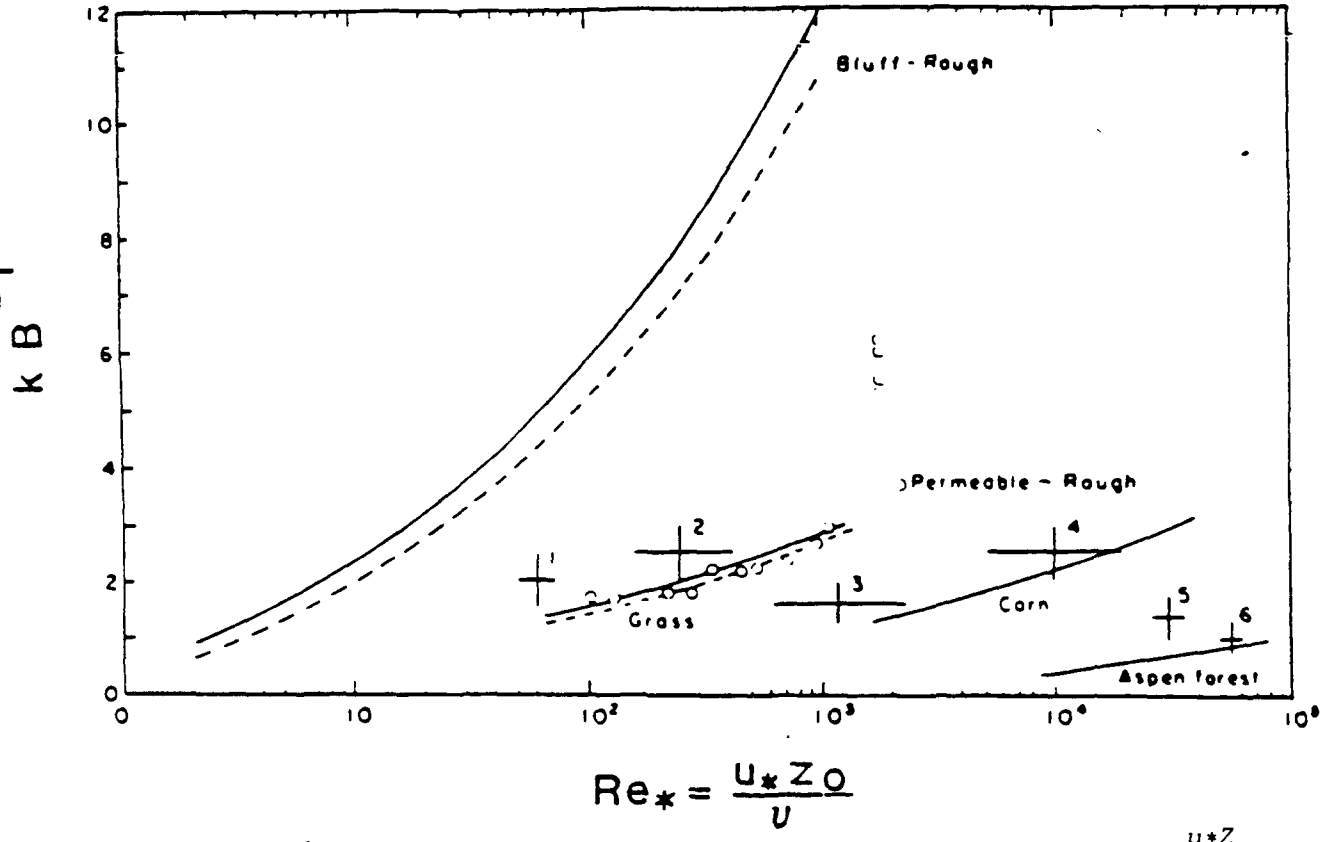

Figure 4. kB^{-1} is a function of the roughness Reynolds number, $Re* = \frac{u*Z_o}{\nu}$ (adapted from W. Brutsaert, 1984, Evaporation in the Atmosphere, D. Reidel Publishing Company, Dordrecht).

3.3 Downward Long-Wave Radiation

Gates (1965) offers an expression for downward long-wave radiation for clear skies based on an empirical relationship by Swinbank (1963).

$$R_{L\downarrow} = -17.09 + 1.195\ \sigma\ T_r^4\ , \tag{31}$$

where R is in milliwatts per centimeter^2, $\sigma = 5.6697\ X\ 10^{-9}$, and T_r the reference level temperature is in degrees kelvin. Paltridge and Platt (1976), in turn, suggest an addition to equation (31) to account for clouds, giving a total expression of

$$R_{L\downarrow} = -17.09 + 1.195\ \sigma\ T_r^4 + 0.3\ \epsilon_c\ \sigma\ T_c^4\ (cc)\ , \tag{32}$$

where ϵ_c, given in table 4, is the emissivity of the cloud base and T_c is the temperature of the cloud base in degrees kelvin. Having an estimate of the cloud height one can approximate T_c, assuming an average of the dry and moist adiabatic lapse rate.

TABLE 4. MEAN SHORT-WAVE PLANETARY ALBEDO, α_{ci}, AND LONG-WAVE FLUX EMISSIVITY, ϵ_{ci}

Cloud Level	Cloud Type	α_{ci}	ϵ_{ci}
1	Cirrus	0.35	0.3
2	Altocumulus-altostratus	0.55	0.9
3	Low cloud 2	0.60	1.0
4	Low cloud 1	0.50	1.0

From the above equations we can compute the first estimate of net radiation, which is then divided into sensible heat, latent heat, and ground heat. For dry, cloudless conditions we assume that the latent heat is zero. To complete the energy balance equation we also need a method for estimating ground heat flux.

3.4 Ground Heat Flux

In our initial formulations we used an equation by Angus-Leppan (1971). Through trial and error using measured flux data we found it necessary to make major changes to that formulation, resulting in

$$G = - G^{*} + \left(T_g - T_{gn} \right) K_o \sin \left\{ \frac{\pi}{12} \left(T - t_n \right) \right\}, \tag{33}$$

where

$$G^{*} = \left[T_g \left(t_n + 2 \right) - T_{gn} \right] K_o \sin \left\{ \pi / 12 \left[\left(t_n + 2 \right) - t_n \right] \right\}. \tag{34}$$

T_{gn} = ground temperature during adiabatic conditions (approximately 1 h after sunrise)

t_n = time (relative to midnight) of adiabatic conditions

$K_o = \frac{Ks}{2\sqrt{K}}$ for soil type and wetness (table 5, Angus-Leppan 1971)

Ks = thermal diffusivity

K = thermal conductivity

TABLE 5. AVERAGE THERMAL PROPERTIES OF SOILS AND SNOW

$$K_o = \frac{Ks}{2\sqrt{K}}$$

Material	State	Water* Content	Ks	K
Sand	Dry	0.0	0.7	2.3
	Moist	0.2	4.2	8.4
	Saturated	0.4	5.2	7.4
Clay	Dry	0.0	0.6	2.0
	Moist	0.2	2.8	5.6
	Saturated	0.4	3.8	5.4
Peat	Dry	0.0	0.14	0.25
	Moist	0.4	0.7	0.9
	Saturated	0.8	1.2	1.0
			Porosity+	
Snow	Fresh	0.95	0.15	3.0
	-	0.8	0.32	1.6
	Compacted	0.5	1.7	3.4

*Volume of water per unit volume of soil
+Volume of pore space per unit volume

(After van Wijk, Physics of plant environment, North Holland 1963)

Equation (34) implies that the ground heat flux is zero approximately 2 h after the neutral period and approximately 3 h after sunrise.

We now introduce formulations by Woolf (1968) that we used to approximate the time of sunrise and sunset. These are followed by our method for computing the morning neutral time. The solar hour angle H' that relates to sunrise and sunset is

$$H' = \arccos \left\{ \frac{\sin A - \sin \phi \sin D}{\cos \phi \cos D} \right\} \qquad (35)$$

where ϕ is the latitude of the site, D is the solar declination angle (see equation (8)) and A is the sunrise/sunset solar elevation angle. At ground level Woolf sets A = -0.9 degree. H' in equation (35) is in degrees, but can be transformed into hours by dividing by 15.

$$H'(^\circ) = 15\ (T - M) - \eta \qquad (36)$$

where T is Greenwich mean time (GMT) and M is the time of the sun's passage over the meridian.

The solar day extends from $M - H'$ to $M + H'$, and hence sunrise time is $M - H'$ and sunset time is $M + H'$.

We also require the time after sunrise when the lower atmosphere is in a neutral state, that is, adiabatic, or when H = 0. This time is designated t_n and is referenced to midnight. First we note that for $t = t_n$, $G = -G^*$ and that G^* remains

$$G^* = [T_g\ (t_n + 2) - T_{gn}]\ K_o \sin \{ \pi/12\ [\ (t_n + 2) - t_n\ ] \} . \tag{37}$$

For very dry soil $L'E \doteq 0$ at t_n.

$$Hence,\ since\ R_n = H + L'E + G \tag{38}$$

R_n reduces to

$$R_n = G = -G^* = [\ T_g\ (t_n + 2) - T_{gn}\ ]\ K_o \sin \{ \pi/12\ [\ (\ t_n + 2\ ) - t_n\ ] \} \tag{39}$$

where K_o is evaluated for dry soil.

Since

$$R_N = (\ 1 - \alpha\ )\ R_{S\downarrow} - (R_{L\uparrow} - R_{L\downarrow}) , \tag{40}$$

we obtain, by equating equations (39) and (40),

$$[T_g\ (t_n + 2) - T_{gn}]\ K_o \sin \left\{ \frac{\pi}{12}\ ((t_n + 2) - t_n) \right\} = -\ (1 - \alpha)\ R_{S\downarrow} + (R_{L\uparrow} - R_{L\downarrow}) . \tag{41}$$

For neutral conditions we approximate $T_g = T_{gn}$ using the formulation

$$T_{gn} = T_{rn} + \Gamma_a\ (z_r - z_h) , \tag{42}$$

where T_r is the reference level, (z_r) is temperature, and Γ_a is the adiabatic lapse rate.

Knowing T_{gn} and T_{rn} one can compute $R_{L\uparrow}$ *and* $R_{L\downarrow}$ using equations (21) and (31); that is,

$$R_{L\uparrow} = \epsilon_g\ \sigma\ T_g^4 + (\ 1 - \epsilon_g\ )\ R_{L\downarrow} , \tag{43a}$$

and

$$R_{L\downarrow} = -17.09 + 1.195\ \sigma\ T_r^4 . \tag{43b}$$

Finally, since $R_{S\downarrow}$ can be evaluated as a function of time, one can find the time t_n that satisfies equation (41). This we define as the neutral time for dry soil, which is approximately 1 h after sunrise.

For moist or saturated soil, the above procedure is modified to allow for nonzero values of $L'E$ as follows.

The latent heat flux $L'E$ can be written as

$$L'E = -L' \rho u^* q^* , \tag{44}$$

where u^* (equation (24)) is the friction velocity, ρ is the air density, L' is the latent heat of vaporization of water, and q^* is the specific humidity scaling length defined by

$$\frac{\partial q}{\partial z} = \frac{q^*}{kz} \phi_q , \tag{45}$$

where k is Karman's constant, and

$$\phi_q = \left[1 - 15 \frac{z}{L}\right]^{-1/2} \quad \text{for unstable conditions,} \tag{46a}$$

$$\phi_q = 1 + 5 \frac{z}{L} \quad \text{for stable conditions,} \tag{46b}$$

$$\phi_q = 1 \quad \text{for neutral conditions,} \tag{46c}$$

The integral of equation (45) is

$$q - q_r = \frac{q^*}{k} \left[\ln \left(\frac{\phi_q^{-1} - 1}{\phi_q^{-1} + 1}\right)\right] \Big|_{z_h}^{z-d} \quad \text{for unstable conditions,} \tag{47a}$$

$$q - q_r = \frac{q^*}{k} \left[\ln \left(\frac{\phi_q^{-1} - 1}{\phi_q^{-1} + 1}\right)\right] \Big|_{z_h}^{z-d} \quad \text{for stable conditions,} \tag{47b}$$

and

$$q - q_{z_h} = \frac{q^*}{k} \ln \frac{z}{z_h} \quad \text{for neutral conditions.} \tag{47c}$$

From the Clausius-Clapyreon equation we can write

$$q = 3.8 \times 10^{-3} f \exp\left\{K \left[\frac{1}{273.16} - \frac{1}{T}\right]\right\}, \tag{48}$$

where f is relative humidity and $K' = 5.44 \times 10^3$.

For neutral conditions the reference level and ground level q can be expressed as

$$q_{r\,n} = 3.8 \times 10^{-3} f_{r\,n} \exp\left\{K'\left(\frac{1}{273.16} - \frac{1}{T_{r\,n}}\right)\right\}, \qquad (49a)$$

and

$$q_{g\,n} = 3.8 \times 10^{-3} f_{r\,n} \exp\left\{K'\left(\frac{1}{273.16} - \frac{1}{T_{g\,n}}\right)\right\}. \qquad (49b)$$

Because of the very small difference between $T_{r\,n}$ and T_{gn}, on the order of 0.02°, equation (49) can be differenced to give an approximation for equation (47c); that is,

$$8q_{g\,n} - q_{r\,n} = -3.8 \times 10^{-3} \exp\left\{K'\left(\frac{1}{273.16} - \frac{1}{T_{r\,n}}\right)\right\} \cdot (f_{g\,n} - f_{r\,n}). \qquad (50)$$

Using equation (47c),

$$q^* \doteq \frac{-3.8 \times 10^{-3}\, k}{\ln \frac{Z_r}{Z_h}} (f_{gn} - f_{r\,n}) \exp\left\{K'\left(\frac{1}{273.16} - \frac{1}{T_{r\,n}}\right)\right\}. \qquad (51)$$

At this point we have all the equations necessary for computing approximations for R_N, H, and G for dry, cloudless, or moist ground cloudy conditions. The next section provides our step-by-step procedure for computing the sensible and latent heat fluxes using the equations presented above.

4. COMPUTATIONAL PROCEDURE

In this section a flowchart (figure 5) of the computational procedure is followed by a more detailed step-by-step method.

The following are assumed to be known at a geographical site where one wishes to compute estimates of sensible and latent heat fluxes: (1) longitude and latitude of the site; (2) day of year and time of day; (3) reference level (2 m) values of temperature (T_r), pressure (P_r), relative humidity (f_r), and horizontal windspeed (V_r); (4) measure or judgment of cloud cover in tenths and cloud density on a scale of 0 to 3 (3 being most dense); (5) albedo of the soil, including vegetative cover; (6) composition and wetness of the soil (dry, moist, saturated); and (7) estimate of cloud type and height.

Step 1: Compute the elevation angle $\phi_e = 90° - Z$ of the sun at the times of interest using Woolf's (1968) formulations. See step 7.

Step 2: Compute a first approximation of the sensible heat flux H for dry ground and cloudless skies using Angus-Leppan and Brunner (1980); that is,

$$H = 450C\,W \sin \phi_e \quad \text{(for C = W 1 in figure 3).} \qquad (52)$$

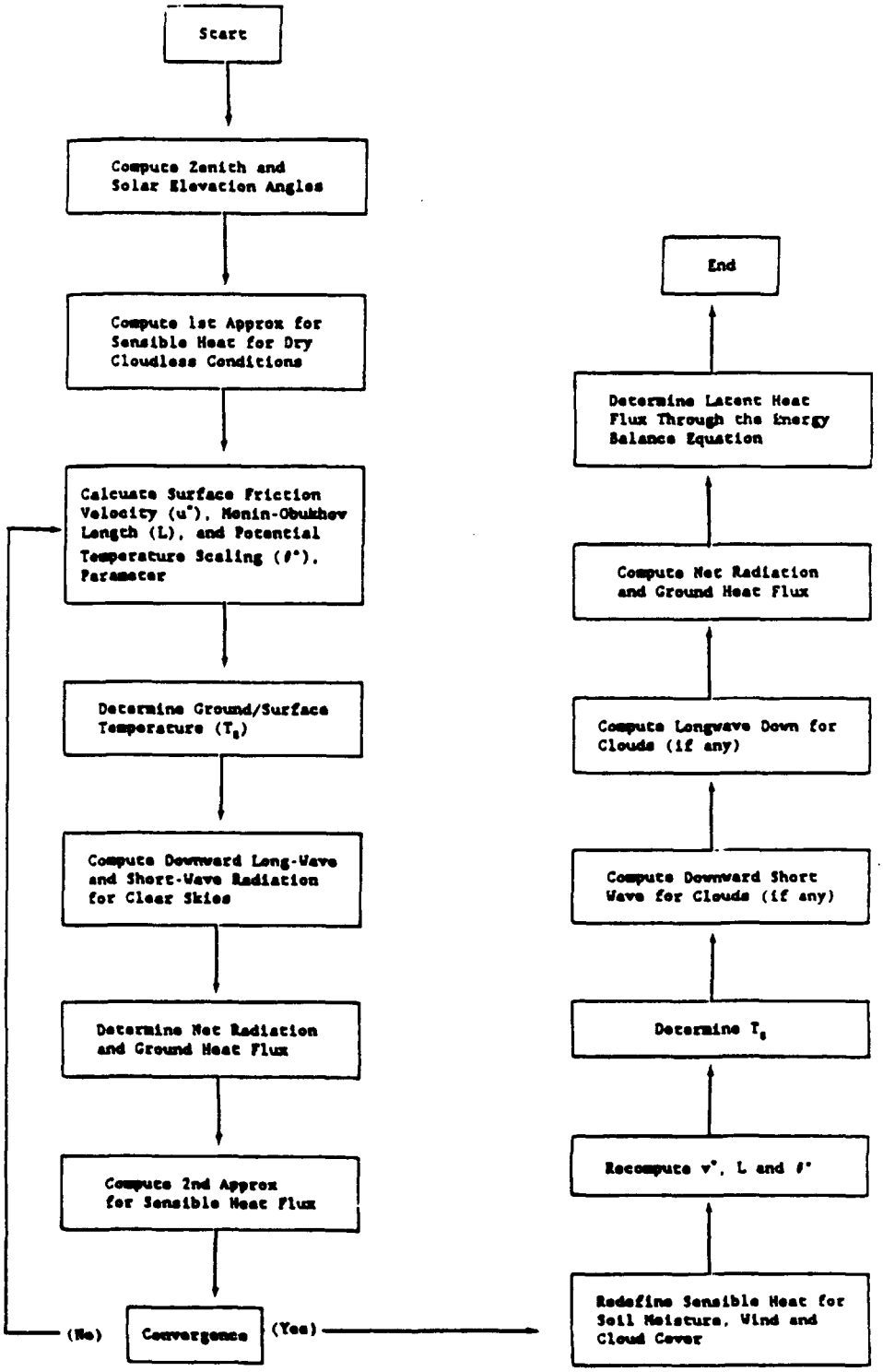

Figure 5. Flowchart of computational procedure.

Step 3: Compute the friction velocity u^* and the Monin-Obukhov length L.

$$u^* = v_r\, k \left\{ \ln\left[\frac{x - 1}{x + 1}\right] + 2 \tan^{-1} x \right\} \Big|_{z_o}^{z-d} ; \tag{53}$$

$$X = \left[1 - 15 \frac{z}{L}\right]^{1/4} ; \tag{54}$$

$$L = -u^{*3}\, C_p\, \rho\, T_r \,/\, kgH , \tag{55}$$

where V_r is the reference level windspeed, k is Karman's constant (0.4), C_p is the specific heat of air, ρ is the air density, T is the temperature at reference height, g is acceleration due to gravity, and Z_o is the roughness length for momentum, where from Liu et al. (1976)

$$\ln(Z_o) = -2.85 + 1.19 \ln Z_e , \tag{56}$$

where Z_e is the height of the roughness element.

Step 4: Compute the potential temperature scaling constant θ^* using

$$\theta^* = u^{*2}\, T_r \,/\, kgL , \tag{57}$$

where for unstable conditions, $T_r = \theta_{vr}$.

Step 5: Knowing T_r, θ^* *and* L, compute the effective temperature T_g at height Z_h (RT modification of Verma (1989)) using

$$T_g = T_r - \frac{\theta^*}{k} \ln\left[\frac{y - 1}{y + 1}\right] \Big|_{z_h}^{z_r-d} , \tag{58}$$

where $y = \left[1 - 15 \frac{z}{L}\right]^{1/2}$ for unstable conditions, and

d = displacement height = $0.7H^*$

$$Z_h = \frac{L}{15} \left\{ 1 - \left[\frac{1 + B^*}{1 - B^*}\right]^2 \right\} ; \tag{59}$$

$$B^* = \left[\frac{y(z - d) + 1}{y(z - d) - 1}\right] \epsilon^{(\,kB^{-1} + A\,)} ; \tag{60}$$

$$A = \left\{ \ln \left[\frac{x - 1}{x + 1} \right] + 2 \tan^{-1} x \right\} \Big|_{z_o}^{z-d} . \quad (61)$$

Z_o = roughness length for momentum over vegetated surface = $0.14H^*$.

H^* = average height of roughness elements.

kB^{-1} = Stanton number, Verma (1989).

Step 6: Compute $R_{L\downarrow} = -17.09 + 1.195\ \sigma\ T_r^4$ where $R_{L\downarrow}$ is in milliwatts per centimeter^{-2} and T_r is in degrees kelvin (Swinbank 1963).

Step 7: Meyers and Dale (1983) compute $R_{s\downarrow}$ for cloudless skies as

$$R_{S\downarrow} = I = I_o\ T_R\ T_g\ T_w\ T_a \cos Z , \quad (62)$$

where I_o is the extraterrestrial flux density at the top of the atmosphere on a surface normal to the incident radiation, Z is the solar zenith angle, and T_i are the transmission coefficients for Rayleigh scattering (R), absorption by permanent gases (g), water vapor (w), and absorption and scattering by aerosols (a).

$$I_o = 1353\ (W\ m^2) \left\{ 1 + 0.034 \cos \left[2\ \pi\ (n' - 1) / 365 \right] \right\} , \quad (63)$$

where n' is the Julian day, and

$$Z = \cos^{-1} (\sin \phi \sin D + \cos \phi \cos D \cos H') , \quad (64)$$

where ϕ is the latitude, D is the declination angle, and H' is the solar hour angle (see step 8).

$$\sin D = \sin (23.4438) \sin \beta . \quad (65)$$

$$\beta\ (^\circ) = \gamma + 0.4087 \sin (\gamma) + 1.8724 \cos (\gamma) - 0.0182 \sin (2\gamma) + 0.0083 \cos (2\gamma) \quad (66)$$

$$\gamma = 279.9348 + d , \quad (67)$$

where d is the angular fraction of a year; that is, d = (Julian day - 1) (360/365.242) (68)

$$T_R\ T_g = 1.021 - 0.084 \left[m\ 949\ P\ x\ 10^{-5} + 0.051 \right]^{1/2} \quad (69)$$

where P is the surface pressure (kPa), and m is the optical air mass at a pressure of 101.3 kPa

$$m = 35 \left(1224 \cos^2 (Z) + 1 \right)^{-1/2} \tag{70}$$

$$T_w = 1 - 0.077 \, (um)^{0.3} \tag{71}$$

where u is the precipitable water vapor (Smith 1966),

$$u = P_o \, W_o \, / \, g \, (\lambda + 1) \ , \tag{72}$$

where P_o is the pressure at the earth's surface, and W_o is the mixing ratio. Values of λ are tabulated in Smith (1966).

$$T_a = x^m, \ \textit{where } x = 0.935 \ . \tag{73}$$

Step 8: Compute sunrise, local noon, and sunset time using Woolf's (1968) formulations. From Woolf the solar hour angle H' that relates to sunrise and sunset is

$$H' = \arccos \left\{ \frac{\sin A - \sin \phi \sin D}{\cos \phi \cos D} \right\} , \tag{74}$$

where ϕ is the latitude, D is the solar declination angle, and A is the sunrise/sunset solar elevation angle. At ground level Woolf sets A = -0.9 degree. H' is in degrees, but is transformed to time in hours by dividing by 15. The solar day extends from $M - H'$ to $M + H'$.

Step 9: Compute $(1 - \alpha) \, R_{s\downarrow}$ using α from Paltridge and Platt (1976).

$$\alpha = \alpha' + (1 - \alpha') \exp \left[-k(90° - Z) \right] , \tag{75}$$

where k = 0.1, Z = zenith angle, and α' is albedo at high solar elevations.

Step 10: Compute $R_{L\uparrow}$ using Yamada (1981)

$$R_{L\uparrow} = \epsilon_g \, \sigma \, T_g^4 + (1 - \epsilon_g) \, R_{L\downarrow} \ . \tag{76}$$

Step 11: Compute net radiation (Steps 1 through 15).

$$R_N = (1 - \alpha) \, R_{S\downarrow} - (R_{L\uparrow} - R_{L\downarrow}) \ . \tag{77}$$

Step 12: Compute $T_g - T_{gn}$ using $T_{gn} = T_{rn} + \gamma_d \, (Z_r - (Z_h + d))$, where T_{gn} is the temperature in degrees kelvin at Z_h, γ_d is the dry adiabatic lapse rate, and T_{rn} is the reference height temperature at the time t_n (relative to midnight) of neutral conditions (see step 13).

Step 13: Compute dry value of G, that is, G_d using a formulation by Rachele and Tunick (see equation 33).

Step 20: Compute $R_{S\downarrow}$ for cloudy skies using Haurwitz (1945).

Step 21: Compute $(1 - \alpha)\, R_{S\downarrow}$.

Step 22: Compute $R_{L\downarrow} = -17.09 + 1.195\ \sigma\ T_r^4 + 0.3\ \epsilon_c\ \sigma\ T_c^4$ (cc) (86)

where $R_{L\downarrow}$ is in milliwatts/centimeter^2, ϵ_c is cloud emissivity, T_c is temperature at cloud base, and cc is tenths of cloud cover.

Step 23: Compute $R_{L\uparrow}$ using the wet value of T_g; that is,

$$R_{L\uparrow} = \epsilon_g\ \sigma\ T_g^4 + (1 - \epsilon_g)\ R_{L\downarrow} \tag{87}$$

Step 24: Compute $R_N = (1 - \alpha)\, R_{S\downarrow} - (R_{L\uparrow} - R_{L\downarrow})$ (88)

Step 25: Compute $T_g - T_{gn}$

Step 26: Compute moist value of G using expression in step 13, when K_o is the moist value in Angus-Leppan (1971).

Step 27: Compute $L'E$ *from* $L'E = R_N - G - H$. (89)

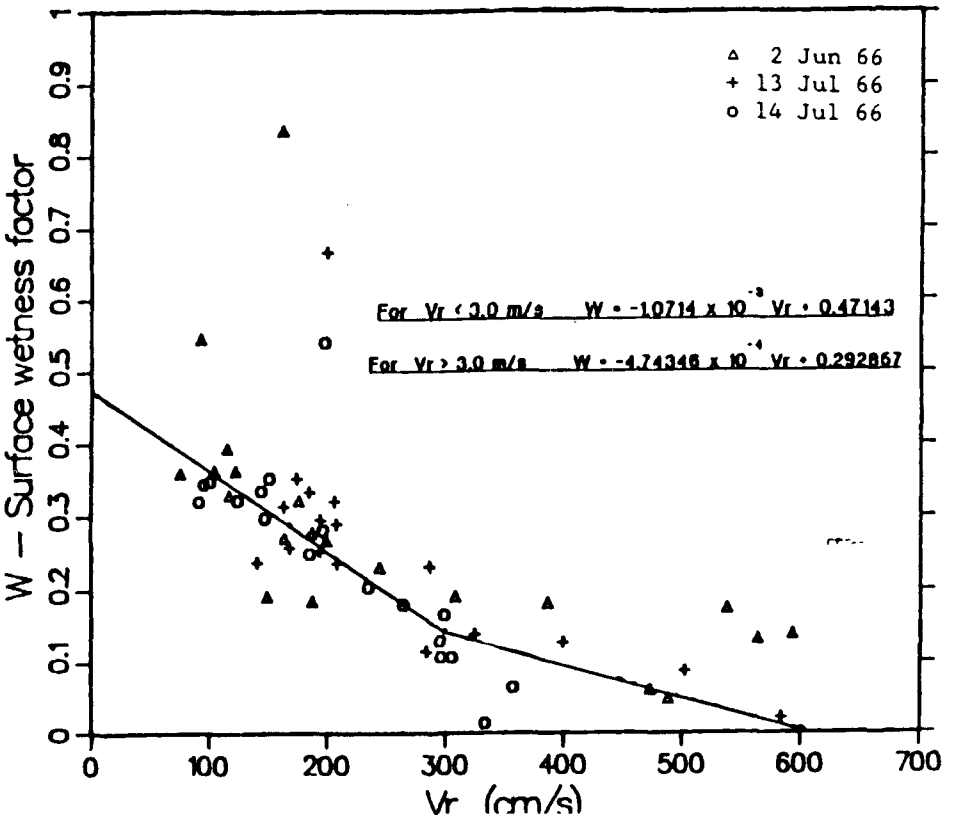

Figure 6. The Rachele/Tunick function $W(V_r)$ (a modified Angus-Leppan and Brunner plot).

5. MODEL RESULTS

The results of this study are based on two sets of measured data (1/2-h averages) collected at Davis, California, during the summer of 1966 (Stenmark and Drury 1970; Brooks et al. 1968; Morgan et al. 1970). The Davis field site, a flat, 5-ha area, at 17 m elevation above sea level, is located about 2 km west of the main portion of the University of California at the Davis Campus, 24 km west of Sacramento, and 113 km northeast of San Francisco. The data were taken during periods when the surrounding fields, were for the most part, crop covered and well irrigated, giving, in effect, homogenous surface conditions with respect to temperature and moisture. Advection effects were considered to be negligible. Profiles of wind, temperature, and moisture were measured with transducers at nine levels from 25 to 600 cm. Raw data were processed to give 1/2-h average profiles.

In addition, 1/2-h values of net radiation and sensible, latent, and soil heat fluxes were available. The terrain at Davis was relatively smooth and covered with fescue grass (average height 10 cm). The soil was assumed to be peat and was moist. Both sets of data were collected during cloudless sky conditions.

Figure 7 shows the 1/2-h average values of reference level temperature, relative humidity, and windspeed for the 2 days. Figures 8, 9, and 10 shows the measured and model values of sensible, latent, and ground heat fluxes for both days. Figure 11 shows the measured and model net radiation for both days. Figure 12 shows the results for the numerically approximated optical turbulence structure parameter (in the visible) for both days using measured and modeled fluxes for inputs.

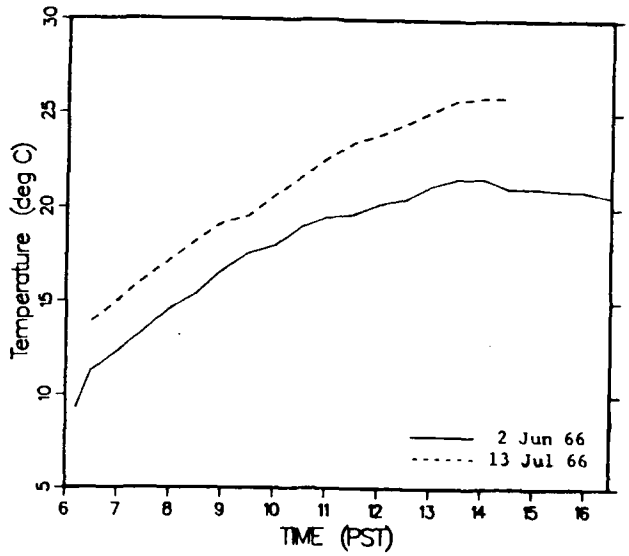

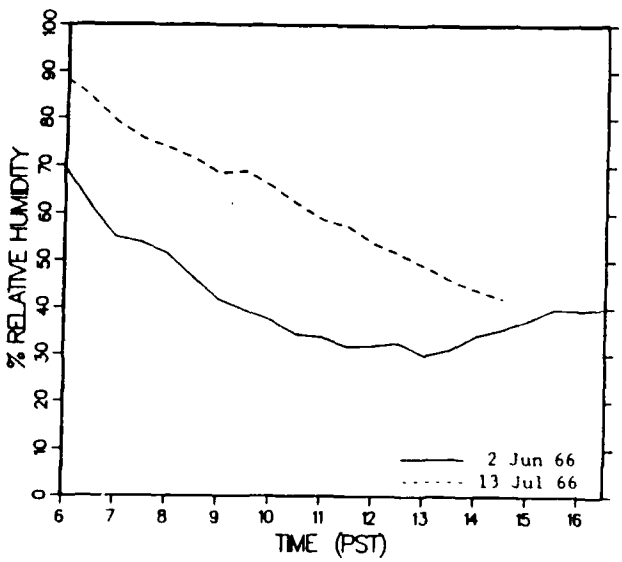

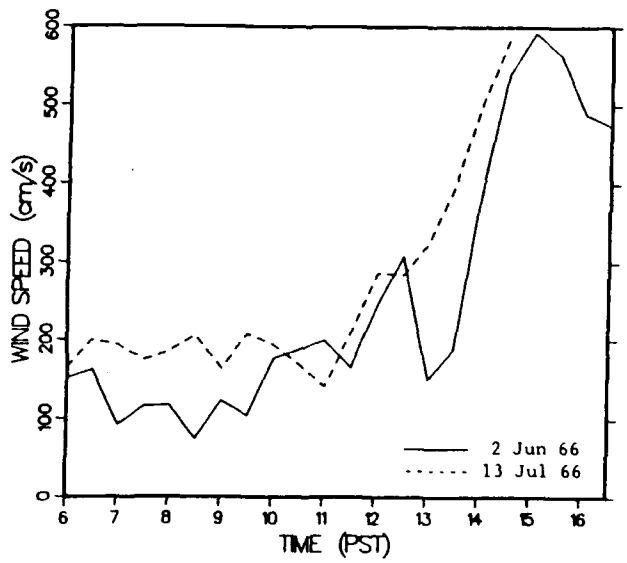

Figure 7. 1/2-h average values of reference level (2 m) temperature, relative humidity, and windspeed (Davis, CA, data).

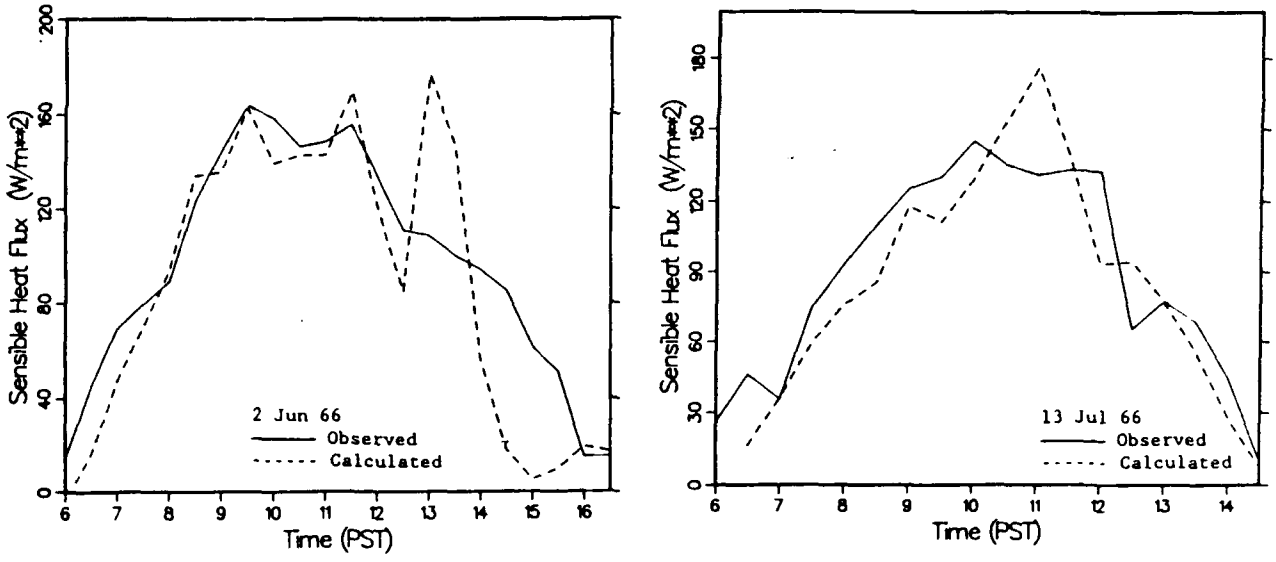

Figure 8. Measured (solid line) and modeled (dashed line) values of sensible heat for Davis, CA, data.

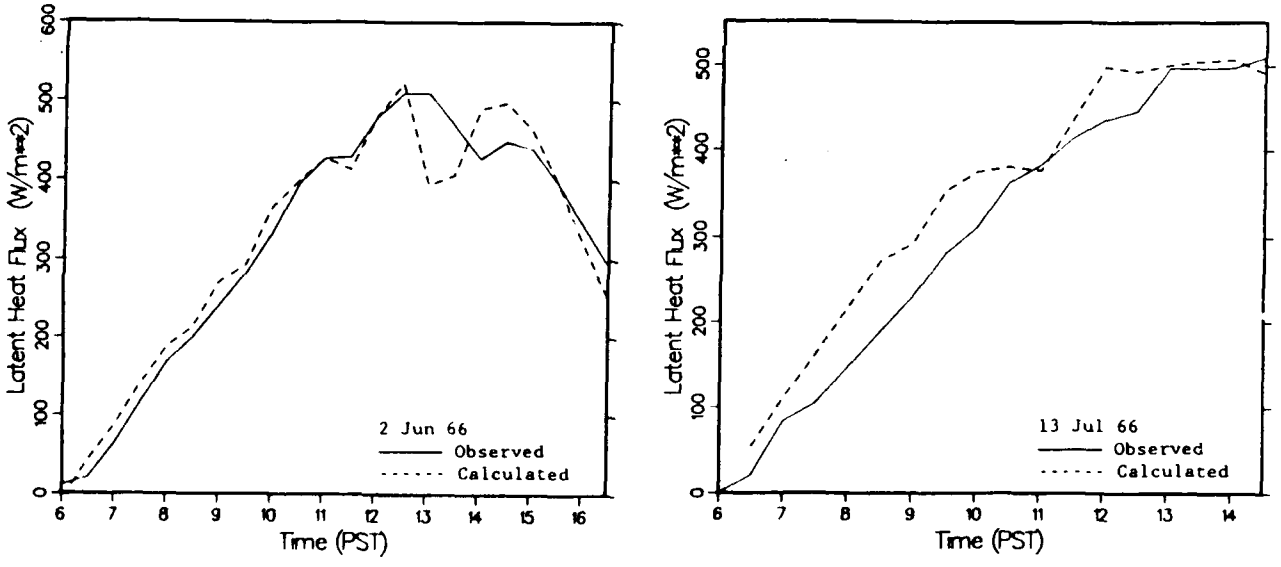

Figure 9. Measured (solid line) and modeled (dashed line) values of latent heat for Davis, CA, data.

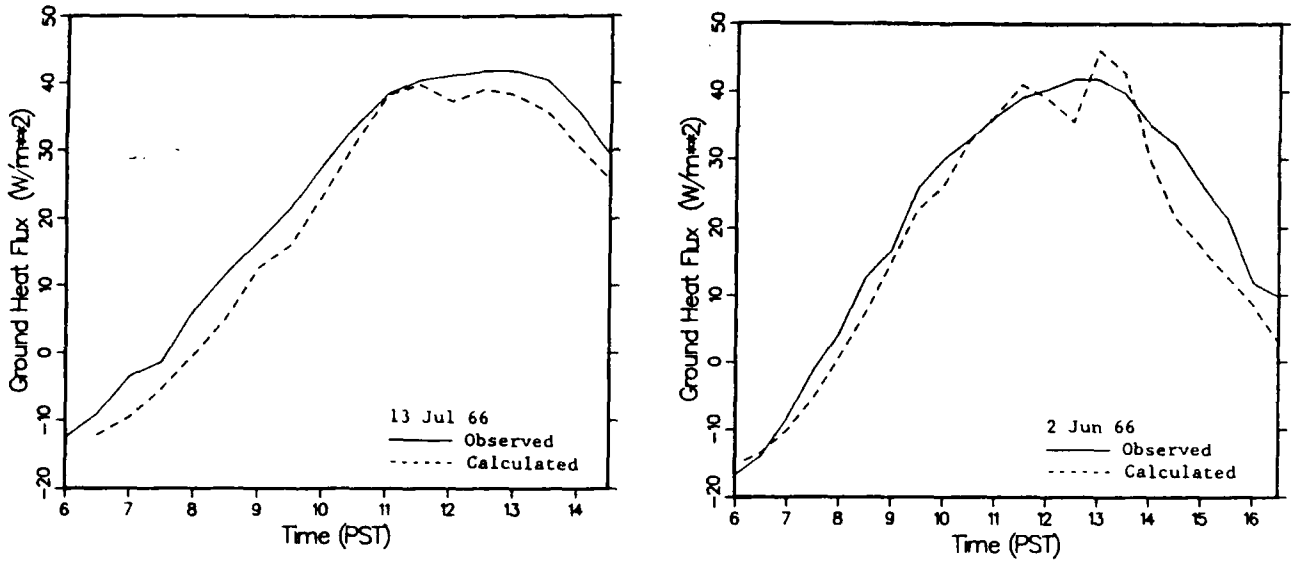

Figure 10. Measured (solid line) and modeled (dashed line) values of ground heat flux for Davis, CA, data.

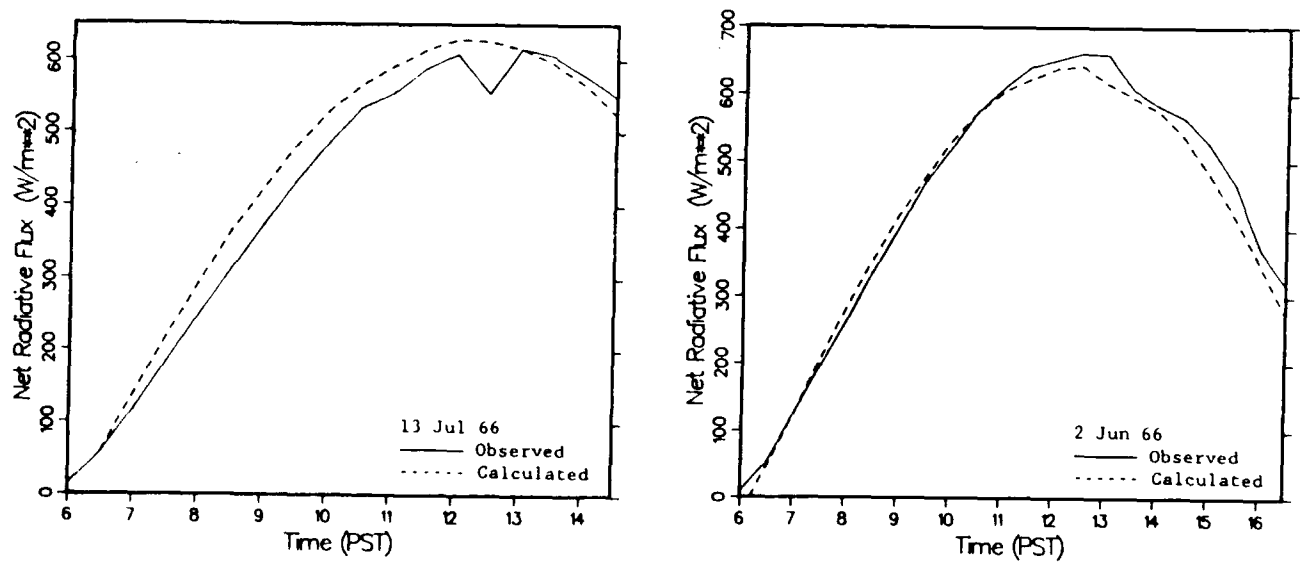

Figure 11. Measured (solid line) and modeled (dashed line) values of net radiative flux for Davis, CA, data.

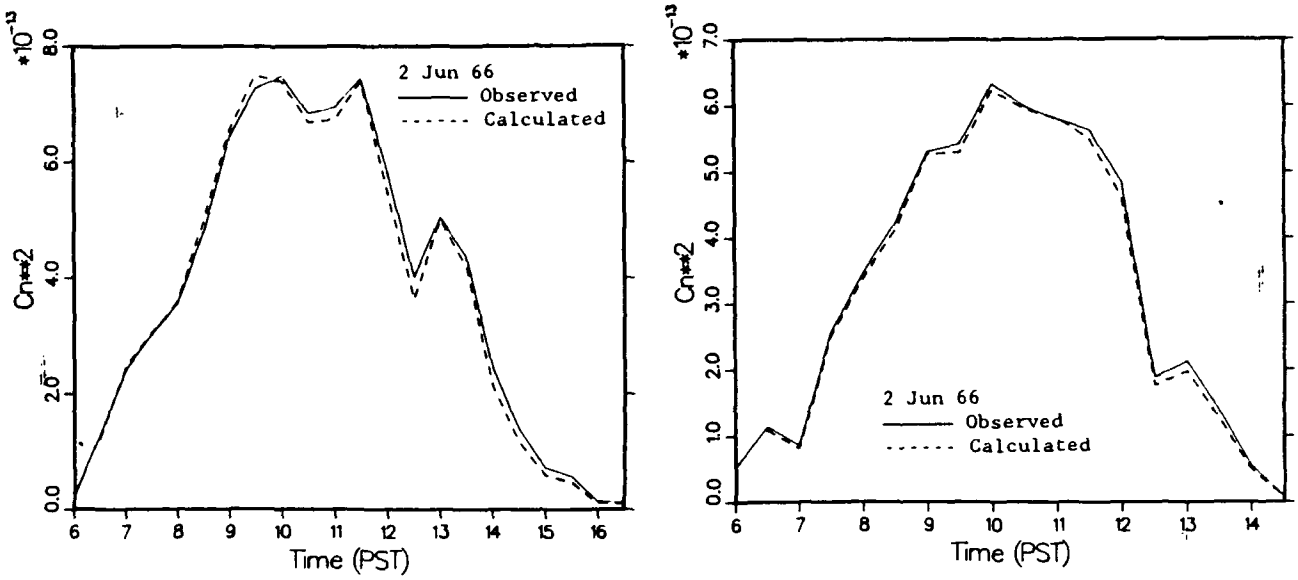

Figure 12. The optical turbulence structure parameter, C_n^2, for visible wavelengths for Davis, CA, data. Measured fluxes as input (solid line), modeled fluxes as input (dashed line).

6. DISCUSSION

Figure 7 shows that day 7-13-66 had both higher temperature and surface relative humidity values than day 6-2-66.

A discrepancy appears in both halves in figure 8 regarding sensible heat flux estimations. The figure shows that by early afternoon the observed sensible heat begins to decline in magnitude; however, an upward spike appears in the modeled results. This is a situation where the observed wind velocity actually decreases (from 2 to 3 m/s to 1.5 m/s); however, the observed heat flux does not respond by growing larger in magnitude. Our model, however, forces a jump in sensible heat when a jump in windspeed occurs.

Since the estimated latent heat flux is a result of the energy balance equation, some discrepancy therefore appears in the early afternoon in figure 9 for day 6-2-66. For day 7-13-66 the net radiation estimates (figure 11) are responsible for the discrepancies seen in the morning hours.

Finally the ground heat flux estimates seem to be in very good agreement with the observations, considering the complexity of the problem.

7. SUMMARY AND CONCLUSIONS

The purpose of this study was to determine the feasibility of structuring a radiation/energy balance model that would yield estimates of sensible and latent heat fluxes, suitable for imagery and EM propagation assessments, research, and applications, when constrained to require atmospheric measurement of temperature, pressure, relative humidity, and wind at a reference height (about 2 m) only.

The model presented satisfies the above constraints; however, one must also know the day of the year, time of day, longitude and latitude of the site of interest, judgment of soil type and moisture (dry, moist, saturated), and cloud characteristics (tenths of cloud cover, density, cloud type, and approximate height).

The model is a composite of formulations, some purely physical and well founded, others semiempirical, and a few that are strictly empirical. Our major contributions include formulations for estimating the effect of wind on the sensible heat flux; an expression for estimating ground heat flux; a modification of Verma's expression for the computation of the roughness length of temperature; and, most critically, tying together all the formulations and establishing a calculation procedure.

The two cases presented in this report were restricted to daytime cloudless conditions using data from Davis, California. Results are most encouraging for determining qualitative estimates of C_n^2 throughout the day over fescue grass.

Finally, it is only fair to say that the model should be used and refined for barren surfaces and other vegetative cover. A joint effort with the U.S. Department of Agriculture is currently planned.

LITERATURE CITED

Andreas, Edgar L., 1988, "Estimating C_n^2 Over Snow and Sea Ice from Meteorological Data," J Opt Soc Am, 5:481-495.

Angus-Leppan, P. V., and F. K. Brunner, 1980, "Atmospheric Temperature Models for Short-Range EDM," The Canadian Surveyor, 34(2):153-165.

Angus-Leppan, P. V., 1971, "Meteorological Physics Applied to the Calculation of Refraction Corrections," in Proceedings of the Conference of Commonwealth Survey Officers, Cambridge, England, pp 107-111.

Atwater, M. A., and P. Brown, 1974, "Numerical Calculation of the Latitudinal Variation of Solar Radiation for an Atmosphere of Varying Opacity," J Appl Meteorol, 13:289-297.

Brooks, F. A., et al., 1968, Analysis in Transfers off Energy, Momentum and Moisture Near the Ground, ECOM-66-G26-F, U.S. Army Electronics Command, Atmospheric Sciences Laboratory, Fort Huachuca, Arizona.

Brutsaert, W., 1984, Evaporation in the Atmosphere, D. Reidel Publishing Company, Dordrecht.

Campbell, G. S., 1985, Soil Physics with Basic: Transport Models for Soil-Plant Systems, Elsevier Publishing Company, Amsterdam, Oxford, New York, Tokyo.

Campbell, G. S., 1977, An Introduction to Environmental Biophysics, Springer Verlag, New York.

Carson, D. J., 1987, "An Introduction to the Parameterization of Land-Surface Processes: Part 1. Radiation and Turbulence," Meteorological Magazine No. 1381, 116:229-242.

Danard, M., G. Lyv, and G. MacGillivray, 1984, "A Mesoscale Bulk Model of the Atmospheric Boundary Layer," Atmospheric Dynamics Corporation Report, Victoria, British Columbia, Canada.

Fried, D. L., 1967, "Propagation of a Spherical Wave in a Turbulent Medium," J Opt Soc Am, 57:175-180.

Gates, D. M., 1965, "Radiant Energy, Its Receipt and Disposal," in Meteorological Monographs, Agricultural Meteorology, vol 6, no 28, American Meteorological Society, Boston, MA, pp 1-26.

Haurwitz, B., 1945, "Insolation in relation to cloudiness and cloud density," J Meteorol, 2(3):154-166.

Hill, R. J., 1989, "Implications of Monin-Obukhov Similarity Theory for Scalar Quantities," J Atmos Sci, 46:2236-2244.

Houghton, H. G., 1954, "On the Annual Heat Balance of the Northern Hemisphere," J Meteorol, 11:1-9.

Kondratyv, K. Ya, 1969, Radiation in the Atmosphere, Academic Press, New York, and London, p 912.

Liu, M. et al., 1976, "The Chemistry Dispersion and Transport of Air Pollutants Emitted From Fossil Fuel Plants in California: Data Analysis and Emission Impact Model," PB-264-822, National Technical Information Center, Springfield, VA, pp 136-140.

McDonald, J. E., 1960, "Direct Absorption of Solar Radiation by Atmospheric Water Vapor," J Meteorol, 17:319-328.

Meyers, T. P, and R. F. Dale, 1983, "Predicting Daily Insolation With Hourly Cloud Height and Coverage," J Climate and Appl Meteorol, 22:537-545.

Miller, W. B., and J. C. Ricklin, 1990, "A Module for Imaging Through Optical Turbulence, IMTURB," ASL-TR-0221-27, U.S. Army Atmospheric Sciences Laboratory, White Sands Missile Range, NM.

Morgan, D. L., et al., 1970, Evaporation From an Irrigated Turf Under Advection of Dry Air at Davis, California, ECOM-68-G10-1, U.S. Army Electronics Command, Atmospheric Sciences Laboratory, Fort Huachuca, Arizona.

Paltridge, G. W. and C. M. R. Platt, 1976, Radiative Processes in Meteorology and Climatology, Elsevier Scientific Publishing Company, Amsterdam, Oxford, New York.

Panofsky, H. A., 1968, "The Structure Constant for the Index Refraction in Relation to the Gradient of Index of Refraction in the Surface Layer," J Geophys Res, 73(18):6047-6049.

Penman, H. L., 1948, "Natural Evaporation From Open Water Bare Soil and Grass," in Proceedings of the Royal Society, London, 193:120-145.

Pielke, R. A., 1984, Mesoscale Meteorological Modeling, Academic Press, Orlando, San Diego, San Francisco, New York, London, Tokyo, Toronto, Montreal, Sydney.

Smith, W. L., 1966, "Note on the Relationship Between Total Precipitable Water and Surface Dew Point," J Appl Meteorol, 5:726-727.

Stenmark, E. B., and L. D. Drury, 1970, Micrometeorological Field Data From Davis, California 1966-67, Runs Under Non-Advective Conditions, ECOM-6051, U.S. Army Electronics Command, Atmospheric Sciences Laboratory, Fort Huachuca, AZ.

Swinbank, W.C., 1963, "Longwave Radiation From Clear Skies," Quart J Roy Meteorol Soc, 89:339-348.

Tatarski, V. I., 1961, Wave Propagation in a Turbulent Medium, McGraw-Hill Book Company, Incorporated, New York - Toronto - London.

Verma, S. B., 1989, "Aerodynamic Resistances to Transfers of Heat, Mass, and Momentum," Estimation of Areal Evapotranspiration (Proceedings of a Workshop held in Vancouver, BC, Canada, August 1987) IAHS Publication No. 177.

Webb, E. K., 1984, "Temperature and Humidity Structure in the Lower Atmosphere," Geodetic Refraction - Effects of Electromagnetic Wave Propagation Through the Atmosphere, F. K. Brunner, ed, Springer Publishing, Berlin, Heidelberg, New York, Tokyo, pp 85-141.

Wesely, M. L., 1976, "The Combined Effect of Temperature and Humidity Fluctuations on Refractive Index," J Appl Meteorol, 15:43-49.

Woolf, H. M., 1968, "On the Computation of Solar Elevation Angles on the Determination of Sunrise and Sunset Times," National Meteorological Center, Environmental Sciences Services Administration, Hillcrest Heights, MD.

Wyngaard, J. C., 1973, "On Surface Layer Turbulence," In Workshop on Micrometeorology, D. A. Haugen (ed) American Meteorological Society, Boston, MA, pp 101-149.

Yamada, T., 1981, "A Numerical Study of Turbulent Air Flow In and Above Forest Canopy," Journal of the Meteorological Society of Japan, 60(1):439-454.

DISTRIBUTION LIST FOR PUBLIC RELEASE

Commandant
U.S. Army Chemical School
ATTN: ATZN-CM-CC (S. Barnes)
Fort McClellan, AL 36205-5020

Commander
U.S. Army Aviation Center
ATTN: ATZQ-D-MA
Mr. Oliver N. Heath
Fort Rucker, AL 36362

Commander
U.S. Army Aviation Center
ATTN: ATZQ-D-MS (Mr. Donald Wagner)
Fort Rucker, AL 36362

NASA/Marshall Space Flight Center
Deputy Director
Space Science Laboratory
Atmospheric Sciences Division
ATTN: E501 (Dr. George H. Fichtl)
Huntsville, AL 35802

NASA/Marshall Space Flight Center
Atmospheric Sciences Division
ATTN: Code ED-41
Huntsville, AL 35812

Deputy Commander
U.S. Army Strategic Defense Command
ATTN: CSSD-SL-L
Dr. Julius Q. Lilly
P.O. Box 1500
Huntsville, AL 35807-3801

Commander
U.S. Army Missile Command
ATTN: AMSMI-RD-AC-AD
Donald R. Peterson
Redstone Arsenal, AL 35898-5242

Commander
U.S. Army Missile Command
ATTN: AMSMI-RD-AS-SS
Huey F. Anderson
Redstone Arsenal, AL 35898-5253

Commander
U.S. Army Missile Command
ATTN: AMSMI-RD-AS-SS
B. Williams
Redstone Arsenal, AL 35898-5253

Commander
U.S. Army Missile Command
ATTN: AMSMI-RD-DE-SE
Gordon Lill, Jr.
Redstone Arsenal, AL 35898-5245

Commander
U.S. Army Missile Command
Redstone Scientific Information Center
ATTN: AMSMI-RD-CS-R/Documents
Redstone, Arsenal, AL 35898-5241

Commander
U.S. Army Intelligence Center and Fort Huachuca
ATTN: ATSI-CDC-C (Mr. Colanto)
Fort Huachuca, AZ 85613-7000

Northrup Corporation
Electronics Systems Division
ATTN: Dr. Richard D. Tooley
2301 West 120th Street, Box 5032
Hawthorne, CA 90251-5032

Commander - Code 3331
Naval Weapons Center
ATTN: Dr. Alexis Shlanta
China Lake, CA 93555

Commander
Pacific Missile Test Center
Geophysics Division
ATTN: Code 3250 (Terry E. Battalino)
Point Mugu, CA 93042-5000

Lockheed Missiles & Space Co., Inc.
Kenneth R. Hardy
Org/91-01 B/255
3251 Hanover Street
Palo Alto, CA 94304-1191

Commander
Naval Ocean Systems Center
ATTN: Code 54 (Dr. Juergen Richter)
San Diego, CA 92152-5000

Meteorologist in Charge
Kwajalein Missile Range
P.O. Box 67
APO San Francisco, CA 96555

U.S. Department of Commerce
Mountain Administration Support
Center
Library, R-51 Technical Reports
325 S. Broadway
Boulder, CO 80303

Dr. Hans J. Liebe
NTIA/ITS S 3
325 S. Broadway
Boulder, CO 80303

NCAR Library Serials
National Center for Atmos Rsch
P.O. Box 3000
Boulder, CO 80307-3000

Bureau of Reclamation
ATTN: D: 1200
P.O. Box 25007
Denver, CO 80225

HQDA
ATTN: DAMI-POI
Washinting, D.C. 20310-1067

Mil Asst for Env Sci Ofc of
The Undersecretary of Defense
for Rsch & Engr/R&AT/E&LS
Pentagon - Room 3D129
Washington, D.C. 20301-3080

Director
Naval Research Laboratory
ATTN: Code 4110
Dr. Lothar H. Ruhnke
Washington, D.C. 20375-5000

HQDA
DEAN-RMD/Dr. Gomez
Washington, D.C. 20314

Director
Division of Atmospheric Science
National Science Foundation
ATTN: Dr. Eugene W. Bierly
1800 G. Street, N.W.
Washington, D.C. 20550

Commander
Space & Naval Warfare System Command
ATTN: PMW-145-1G (LT Painter)
Washington, D.C. 20362-5100

Commandant
U.S. Army Infantry
ATTN: ATSH-CD-CS-OR
Dr. E. Dutoit
Fort Benning, GA 30905-5090

USAFETAC/DNE
Scott AFB, IL 62225

Air Weather Service
Technical Library - FL4414
Scott AFB, IL 62225-5458

HQ AWS/DOO
Scott AFB, IL 62225-5008

USAFETAC/DNE
ATTN: Mr. Charles Glauber
Scott AFB, IL 62225-5008

Commander
U.S. Army Combined Arms Combat
ATTN: ATZL-CAW (LTC A. Kyle)
Fort Leavenworth, KS 66027-5300

Commander
U.S. Army Combined Arms Combat
ATTN: ATZL-CDB-A (Mr. Annett)
Fort Leavenworth, KS 66027-5300

Commander
U.S. Army Space Institute
ATTN: ATZI-SI (Maj Koepsell)
Fort Leavenworth, KS 66027-5300

Commander
U.S. Army Space Institute
ATTN: ATZL-SI-D
Fort Leavenworth, KS 66027-7300

Commander
Phillips Lab
ATTN: PL/LYP (Mr. Chisholm)
Hanscom AFB, MA 01731-5000

Director
Atmospheric Sciences Division
Geophysics Directorate
Phillips Lab
ATTN: Dr. Robert A. McClatchey
Hanscom AFB, MA 01731-5000

Raytheon Company
Dr. Charles M. Sonnenschein
Equipment Division
528 Boston Post Road
Sudbury, MA 01776
Mail Stop 1K9

Director
U.S. Army Materiel Systems
Analysis Activity
ATTN: AMXSY-MP (H. Cohen)
APG, MD 21005-5071

Commander
U.S. Army Chemical Rsch,
Dev & Engr Center
ATTN: SMCCR-OPA (Ronald Pennsyle)
APG, MD 21010-5423

Commander
U.S. Army Chemical Rsch,
Dev & Engr Center
ATTN: SMCCR-RS (Mr. Joseph Vervier)
APG, MD 21010-5423

Commander
U.S. Army Chemical Rsch,
Dev & Engr Center
ATTN: SMCCR-MUC (Mr. A. Van De Wal)
APG, MD 21010-5423

Director
U.S. Army Materiel Systems
Analysis Activity
ATTN: AMXSY-AT (Mr. Fred Campbell)
APG, MD 21005-5071

Director
U.S. Army Materiel Systems
Analysis Activity
ATTN: AMXSY-CR (Robert N. Marchetti)
APG, MD 21005-5071

Director
U.S. Army Materiel Systems
Analysis Activity
ATTN: AMXSY-CS (Mr. Brad W. Bradley)
APG, MD 21005-5071

Commander
U.S. Army Laboratory Command
ATTN: AMSLC-CG
2800 Powder Mill Road
Adelphi, MD 20783-1145

Commander
Headquarters
U.S. Army Laboratory Command
ATTN: AMSLC-CT
2800 Powder Mill Road
Adelphi, MD 20783-1145

Commander
Harry Diamond Laboratories
ATTN: SLCIS-CO
2800 Powder Mill Road
Adelphi, MD 20783-1197

Director
Harry Diamond Laboratories
ATTN: SLCHD-ST-SP
Dr. Z.G. Sztankay
Adelphi, MD 20783-1197

AFMC/DOW
Wright-Patterson AFB, OH 0334-5000

National Security Agency
ATTN: W21 (Dr. Longbothum)
9800 Savage Road
Ft George G. Meade, MD 20755-6000

U. S. Army Space Technology
and Research Office
ATTN: Brenda Brathwaite
5321 Riggs Road
Gaithersburg, MD 20882

OIC-NAVSWC
Technical Library (Code E-232)
Silver Springs, MD 20903-5000

The Environmental Research
Institute of MI
ATTN: IRIA Library
P.O. Box 8618
Ann Arbor, MI 48107-8618

Commander
U.S. Army Research Office
ATTN: DRXRO-GS (Dr. W.A. Flood)
P.O. Box 12211
Research Trianagle Park, NC 27709

Dr. Jerry Davis
North Carolina State University
Department of Marine, Earth, &
Atmospheric Sciences
P.O. Box 8208
Raleigh, NC 27650-8208

Commander
U. S. Army CECRL
ATTN: CECRL-RG (Dr. H. S. Boyne)
Hanover, NH 03755-1290

Commanding Officer
U.S. Army ARDEC
ATTN: SMCAR-IMI-I, Bldg 59
Dover, NJ 07806-5000

U.S. Army Communications-Electronics
Command Center for EW/RSTA
ATTN: AMSEL-RD-EW-SP
Fort Monmouth, NJ 07703-5303

Commander
U.S. Army Communications-Electronics
Command
ATTN: AMSEL-EW-D (File Copy)
Fort Monmouth, NJ 07703-5303

Headquarters
U.S. Army Communications-Electronics
Command
ATTN: AMSEL-EW-MD
Fort Monmouth, NJ 07703-5303

Commander
U.S. Army Satellite Comm Agency
ATTN: DRCPM-SC-3
Fort Monmouth, NJ 07703-5303

Director
EW/RSTA Center
ATTN: AMSEL-EW-DR
Fort Monmouth, NJ 07703-5303

USACECOM
Center for EW/RSTA
ATTN: AMSEL-RD-EW-SP
Fort Monmouth, NJ 07703-5303

6585th TG (AFSC)
ATTN: RX (CPT Stein)
Holloman AFB, NM 88330

Department of the Air Force
OL/A 2nd Weather Squadron (MAC)
Holloman AFB, NM 88330-5000

PL/WE
Kirtland AFB, NM 87118-6008

Director
U.S. Army TRADOC Analysis Command
ATTN: ATRC-WSS-R
White Sands Missile Range, NM 88002

Rome Laboratory
ATTN: Technical Library RL/DOVL
Griffiss AFB, NY 13441-5700

Department of the Air Force
7th Squadron
APO, NY 09403

AWS
USAREUR/AEAWX
APO, NY 09403-5000

AF Wright Aeronautical Laboratories
Avionics Laboratory
ATTN: AFWAL/AARI (Dr. V. Chimelis)
Wright-Patterson AFB, OH 45433

Commander
U.S. Army Field Artillery School
ATTN: ATSF-F-FD (Mr. Gullion)
Fort Sill, OK 73503-5600

Commandant
U.S. Army Field Artillery School
ATTN: ATSF-TSM-TA
Mr. Charles Taylor
Fort Sill, OK 73503-5600

Commander
Naval Air Development Center
ATTN: Al Salik (Code 5012)
Warminister, PA 18974

Commander
U.S. Army Dugway Proving Ground
ATTN: STEDP-MT-DA-M
Mr. Paul Carlson
Dugway, UT 84022

Commander
U.S. Army Dugway Proving Ground
ATTN: STEDP-MT-DA-L
Dugway, UT 84022

Commander
U.S. Army Dugway Proving Ground
ATTN: STEDP-MT-M (Mr. Bowers)
Dugway, UT 84022-5000

Defense Technical Information Center
ATTN: DTIC-FDAC
Cameron Station
Alexandria, VA 22314

Commanding Officer
U.S. Army Foreign Science &
Technology Center
ATTN: CM
220 7th Street, NE
Charlottesville, VA 22901-5396

Naval Surface Weapons Center
Code G63
Dahlgren, VA 22448-5000

Commander
U.S. Army OEC
ATTN: CSTE-EFS
Park Center IV
4501 Ford Ave
Alexandria, VA 22302-1458

Commander and Director
U.S. Army Corps of Engineers
Engineer Topographics Laboratory
ATTN: ETL-GS-LB
Fort Belvoir, VA 22060

TAC/DOWP
Langley AFB, VA 23665-5524

U.S. Army Topo Engineering Center
ATTN: CETEC-ZC
Fort Belvoir, VA 22060-5546

Commander
Logistics Center
ATTN: ATCL-CE
Fort Lee, VA 23801-6000

Commander
USATRADOC
ATTN: ATCD-FA
Fort Monroe, VA 23651-5170

Science and Technology
101 Research Drive
Hampton, VA 23666-1340

Commander
U.S. Army Nuclear & Cml Agency
ATTN: MONA-ZB Bldg 2073
Springfield, VA 22150-3198